ることで計算量およびメモリ消費を大幅に減少させることができる。また、メモリ上での演算に比べハードディスクへの書き込み速度は遅く、特に要素数の多い結合強度 $a_{\tau}^{(m,n,t)}$ の書き込みを計測と同じ頻度で行うことは難しい。だが今回推定される結合強度の更新頻度は各細胞の発火頻度と同じオーダーであるため、msオーダーの急さな変化は起こりえない。そこで今回は $a^{(m,n,t)}$ の出力レートを10Hzまで下げた。

以上の条件において構築したシステムにおいては計測と並行した実時間での処理が可能であった。

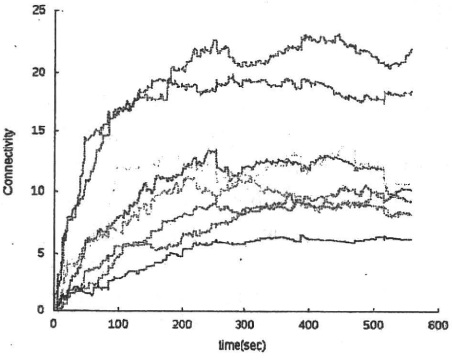

Fig. 1 Time change of estimated connectivity.

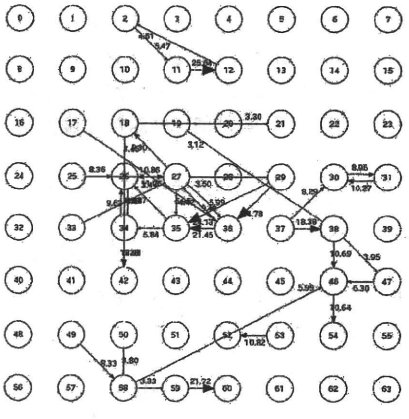

Fig. 2 Estimated network structure on MED.

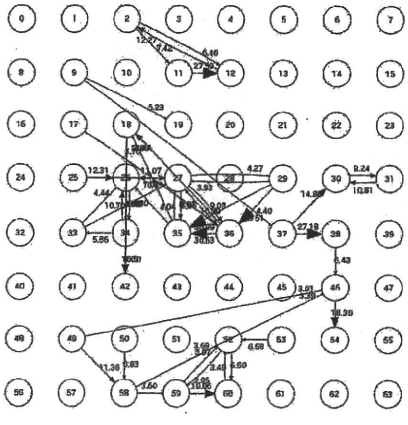

Fig. 3 Network structure estimated half a day after Fig. 2.

3. 実験

3.1 細胞培養・実験条件

ラット胎児(胎生17日)の大脳皮質より得た神経細胞を分散したのち約 1.3×10^{6} Cells/mm^{2} の細胞密度でMEDに播種して培養を行い、MED上に神経細胞ネットワークを再構成させた。培養37日目の神経細胞ネットワークに対し、2.において構築したシステムによる結合推定(K=0.8, σ=10,T=4ms)を行った。

3.2 結果

システムはリアルタイムで動作し、強い結合がいくつか現れ、それらの結合強度はある値付近に収束した。図1にいくつかの結合強度の代表値 $\max_{\tau} a_{\tau}^{(m,n,t)}$ の経時変化を示す。

また、推定されたネットワーク構造を図2に示す。各ノードが計測電極、矢印が結合の向き、矢印先端の大きさ・付記した数字は結合強度の代表値 $\max_{\tau} a_{\tau}^{(m,n,t)}$ を示している。図3は図2の半日後に同条件で同じMEDから推定されたネットワーク構造である。2つのネットワークには共通した構造が見られる。

3.3 考察

本システムの大きな問題として、推定の時間遅れが大きいことがあり、はじめに推定が収束するまでには数分を要している。また、勾配法を用いていることで推定結果が局所解に陥る可能性がある。これらの問題から、パラメータ学習の手法にまだ大きな改善の余地があると考えられる。

4. 結論

リアルタイムで動作する神経細胞ネットワークの結合推定・可視化システムを構築することができ、実際にシステムを使用し推定を行った結果、定常なネットワークの存在を示唆する結果が得られた。今後の課題として、スパイクソーティングの実装や推定手法の改善などリアルタイム性を失わない範囲でのシステムの改良、結合推定に基づいた神経細胞へのフィードバック刺激入力による結合制御などリアルタイム性を生かした応用が挙げられる。

参考文献

[1] 向井嘉崇, 椎名毅, 神保泰彦, "培養神経回路網の自発活動の長期的観測と解析", 電子情報通信学会技術研究報告. OME, 有機エレクトロニクス , Vol. 100, No. 479 , pp. 15-20(2000)

[2] Suguru Kudoh ,Takahisa Taguchi: "Methods to analyze spatio-temporal patterns of electrical activities in living neural networks", SICE Annual Conference, Sapporo, pp.2343-2346 (2004)

[3] Alex J. Cadotte, Thomas B. Demarse, Ping He, Mingzhou Ding: "Causal Measures of Structure and Plasticity in Simulated and Living Neural Networks", PLoS ONE, Vol. 3, Issue 10, e3355 (2008)

[4] Okatan , Wilson , Brown, "Analysing functional connectivity using a network likelihood model of ensemble neural spiking acitivity", Neural computation, Vol. 17, No. 9, pp. 1927—1961 (2005)

ICIC Express Letters
Volume 4, Number 6(A), December 2010

ICIC International ©2010 ISSN 1881-803X
pp. 2183-2188

ESTIMATION OF FINGER JOINT ANGLE BASED ON SURFACE EMG SIGNALS AND ITS SIGNAL SOURCE RECOGNITION

YUKI HOASHI[1], YASUTAKA YAMAMIZU[1], NOZOMU ARAKI[1]
YASUO KONISHI[1], KUNIHIKO MABUCHI[2] AND HIROYUKI ISHIGAKI[1]

[1]Graduate School of Engineering
University of Hyogo
2167 Shosha, Himeji-shi, Hyogo, Japan
araki@eng.u-hyogo.ac.jp

[2]Graduate School of Information Science and Technology
University of Tokyo
7-3-1, Hongo, Bunkyo-ku, Tokyo, Japan

Received March 2010; accepted May 2010

ABSTRACT. *In this study, we proposed a finger joint angle estimation method based on surface electromyography (EMG) signals and their source recognition. We have previously proposed a finger joint angle estimation method based on measured surface EMG signals and a linear model. However, there were some problems with that method. When we estimate 2 or more finger angles by this method simultaneously, the estimated angle of the inactive fingers is not accuate. This is caused by interference of surface EMG signals. To solve this problem, we added the source recognition of surface EMG signals by a Bayesian filter to our angle estimation method. To confirm the effectiveness of our proposed method, we carried out joint angle estimation experiments. In addition, we developed a myoelectric hand simulator that estimates the finger joint angle from surface EMG signals in real time using our proposed method.*
Keywords: Surface EMG signal, Myoelectric hand, Finger joint angle estimation, Bayesian filter

1. **Introduction.** A method for estimating the finger configuration or finger joint angle from electromyography (EMG) signals is important for controlling a myoelectric hand and is being actively researched. Because a myoelectric hand in practical use has few degrees of freedom, to realize a flexible myoelectric hand, it is necessary to accurately estimate the user's intention from EMG signals.

In previous researches, a method was developed for estimating finger posture from surface EMG signals using pattern recognition [1, 2]. A finger joint angle estimation method using surface EMG signals and neural networks has also been developed [3]. Thus, we have already proposed a finger joint angle estimation method using a histogram of surface EMG signals and a linear model [4]. However, there are some problems with our proposed method. In particular, when we estimate 2 or more finger angles simultaneously, the estimated angle of the inactive fingers is not accurate. This is caused by interference of surface EMG signals. To solve this problem, we added source recognition of surface EMG signals by Bayesian filter. Joint angle estimation experiments were carried out to confirm the effectiveness of our proposed method.

2. **Surface EMG Signal Measurement Setup.** First, we describe the surface EMG signal measurement setup for this study. The goal of our study was to estimate the angle of all finger joints from measured surface EMG signals and to control a myoelectric hand by estimated angle. In this study, we consider the estimation of 10 right-hand finger joints, as shown in Figure 1.

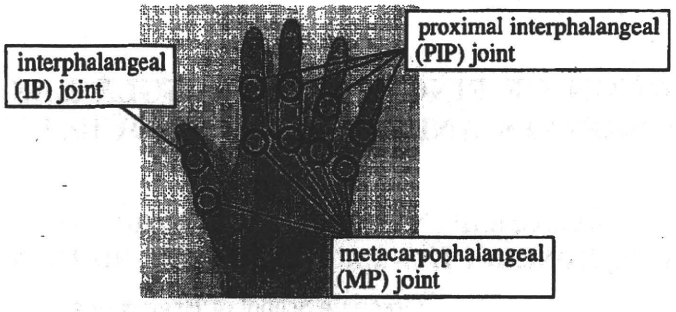

FIGURE 1. Finger joint positions estimated in this study

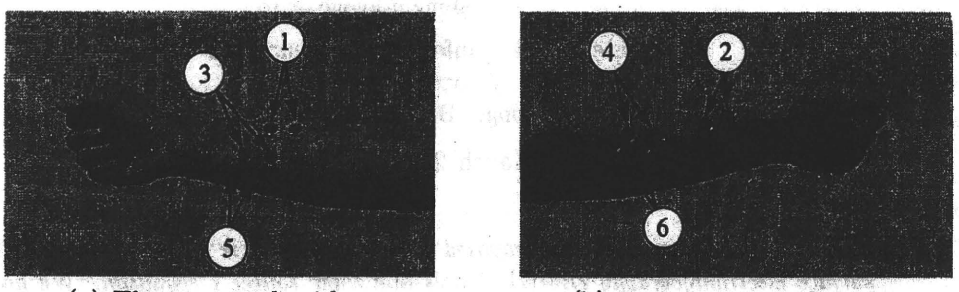

(a) Flexor muscle side (b) Extensor muscle side

FIGURE 2. Electrode position for surface EMG signal measurement

To obtain the relational expression between these angles and surface EMG signals, the angles of the finger joints shown in Figure 1 are measured by rotary potentiometers. Since the finger joint angle is determined by a tension balance between a flexor muscle and an extensor muscle, surface EMG electrodes are applied to 6 positions (3 positions on the flexor muscle side and 3 positions on the extensor muscle side of the forearm) as shown in Figure 2. The sampling frequency of these surface EMG signals is 2000 Hz. Here, the surface EMG signals obtained by a pair of 1-2 electrodes are used for the thumb, 3-4 electrodes are used for the index and middle fingers and 5-6 electrodes are used for the medicinal and little finger, respectively. In the next section, we will describe how the finger joint angles are estimated from these surface EMG signals.

3. Finger Joint Angle Estimation Method Using Histogram of Surface EMG Signals. This section briefly explains our finger joint angle estimation method proposed in [4]. This method is based on a histogram of surface EMG signals. Figure 3(a) shows a sample of original surface EMG signal. In our method, we use only the negative extreme value of this signal as shown in Figure 3(b). This signal value is in the 0 V to -10 V range. We divide this range into 6 classes, and then calculate the frequency of each class using a 0.5 sec. record to create the histogram. Therefore, the obtained histogram has 6 elements $X_1, \ldots, X_6$ that are frequencies of each class.

Now, it is assumed that $\{X_1^f(t), \ldots, X_6^f(t)\}$ is the histogram calculated from the surface EMG signal of a flexor muscle and $\{X_1^e(t), \ldots, X_6^e(t)\}$ is that of an extensor muscle at a time t. Since the finger joint angle is determined by tension balance between a flexor muscle and an extensor muscle, for a certain finger joint angle $\theta(t)$, we assume the following equation.

$$\theta(t) = \theta_0 + \sum_{i=1}^{6} a_i X_i^f(t) + \sum_{j=1}^{6} b_j X_j^e(t) \tag{1}$$

where a_i and b_j are weight coefficients and θ_0 is bias angle. These parameters can be obtained by linear least square method from prepared surface EMG signals and corresponding finger joint angle measured at the same time by a rotary potentiometer. In

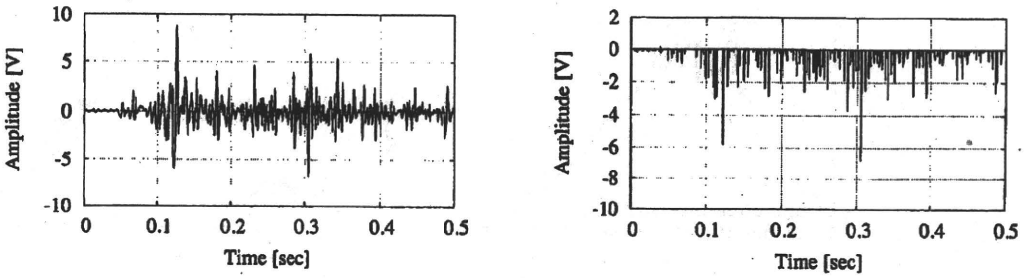

(a) Original surface EMG signal (b) Negative extremal value signal

FIGURE 3. Sample of surface EMG signal and its negative extremal value signal

the estimation step, we calculate a finger joint angle estimator $\hat{\theta}(t)$ from (1) from the histogram of measured surface EMG signals.

To verify the performance of our proposed method, we carried out a finger joint angle estimation experiment. In this experiment, only the index finger was flexed and extended, while the other fingers were not moved. Figure 4 shows the joint angle estimation results for the index finger and middle finger. As shown in Figure 4(a), it is found that our proposed method closely estimates the finger joint angle for the index finger. However, from Figure 4(b), the estimation result diverges sharply from the measured angle of the middle finger, which was inactive. Moreover, all the estimation results are similar in shape. This result is caused by interference of surface EMG signals. To solve this problem, we added source recognition of surface EMG signals by Bayesian filter to our angle estimation method.

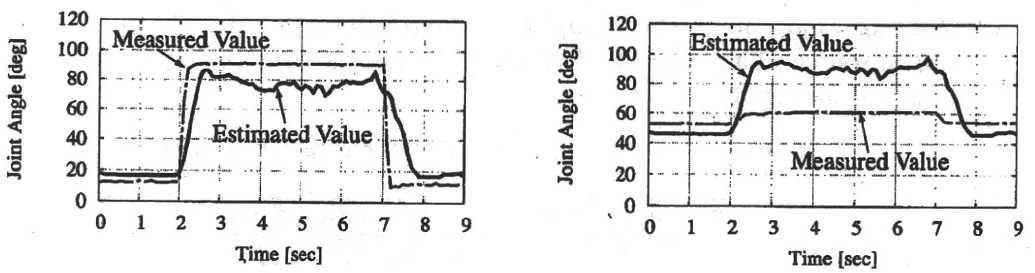

(a) Index finger (active finger) (b) Middle finger (inactive finger)

FIGURE 4. Estimation results of finger joint angle

4. **Signal Source Recognition Using Bayesian Filter.** The problem with our proposed method described in the previous section is caused by interference of surface EMG signals. If an active finger can be recognized from surface EMG signals, we can avoid these errors. Thus, this paper proposes a method for recognizing the signal source of surface EMG signals with a Bayesian filter. A Bayesian filter is a statistical classifier method based on Bayes' theorem and it is known to have high recognition performance [5].

Here, we distinguish the signal source using the fact that the amplitude spectrum of a surface EMG signal has a different distribution for different finger motion. First, the amplitude spectrum of the surface EMG signal is calculated from a 0.3 sec. record. Figure 5(a) shows an example of the amplitude spectrum of a surface EMG signal. Second, as shown in Figure 5(b), we divide the frequency of the obtained amplitude spectrum into 20 regions and calculate the average magnitude in each region. Then, the magnitude of the reduced spectrum is divided into 10 regions. Consequently, the amplitude spectrum of the surface EMG signal is considered as a 10×20 matrix $\mathbf{M}$. The element of $\mathbf{M}$ has a value of 0 or 1. It is 1 if the reduced spectrum is in the divided region indicated by the gray area of Figure 5(b).

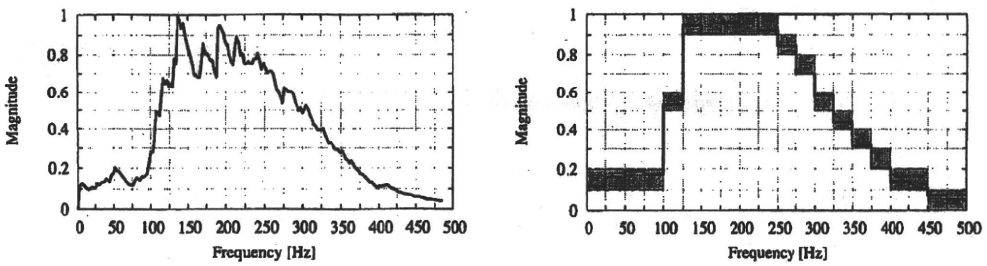

(a) Original spectrum (b) Reduced spectrum

FIGURE 5. Sample of amplitude spectrum of a surface EMG signal

Next, we explain how to create a database to recognize the signal source. Because we measure the surface EMG signals at 6 positions as described in Section 2, it is necessary to calculate 6 amplitude spectrums for one finger motion. Now, for a certain finger motion, we assume that an N-training set of 6 amplitude spectrums are given as a 10×20 matrix $\mathbf{M}_i^j$, $i = 1, \ldots, N$, $j = 1, \ldots, 6$. Then, the hash table for a certain finger motion $\mathbf{H}_j$, $j = 1, \ldots, 6$ is constracted as follows:

$$\mathbf{H}_j = \frac{1}{N} \sum_{i=0}^{N} \mathbf{M}_i^j, \ j = 1, \ldots, 6. \tag{2}$$

The element of this hash table $\mathbf{H}_j$ has range $[0, 1]$. Therefore, the hash table $\mathbf{H}_j$ can be considered as a probability map of the amplitude spectrum of surface EMG signals for a certain finger motion. Then, the set of 6 hash tables $\mathbf{D} = \{\mathbf{H}_1, \ldots, \mathbf{H}_6\}$ is the database of a certain finger motion. In this study, we created 7 databases $\mathbf{D}_k$, $k = 0, \ldots, 6$ to distinguish the signal source. The subscript k of $\mathbf{D}_k$ is the database index and the corresponding finger motion is shown in Table 1.

TABLE 1. Database index and corresponding finger motion

Database index k	Corresponding finger motion
0	hyposthenia state
1	flex action of thumb
2	flex action of index finger
3	flex action of middle finger
4	flex action of medicinal finger
5	flex action of little finger
6	flex action of all fingers

It is assumed that the set of amplitude spectrum matrices $\mathbf{Z} = \{\mathbf{M}^1, \ldots, \mathbf{M}^6\}$ of the surface EMG signals for unknown finger motion are obtained. Then, the probability $P(k|\mathbf{Z})$ that given data $\mathbf{Z}$ are the data of the k-th database and the corresponding finger motion is calculated using Bayes' combining probability as follows:

$$P(k|\mathbf{Z}) = \frac{\prod_{i=1}^{120} \gamma(i)}{\prod_{i=1}^{120} \gamma(i) + \prod_{i=1}^{120} (1 - \gamma(i))} \tag{3}$$

where the probability $\gamma(i)$ is obtained by the following algorithm:

[Calculate the probability $\gamma(k)$]

For database $\mathbf{D}_k = \{\mathbf{H}_1, \ldots, \mathbf{H}_6\}$ and given data $\mathbf{Z} = \{\mathbf{M}^1, \ldots, \mathbf{M}^6\}$, $\gamma(i)$ is calculated as:

$i = 1$ (Initialize)
For $j = 1 : 6$,

For $a = 1 : 10$,
  For $b = 1 : 20$,
    If $\mathbf{M}^j(a,b) == 1$, Then $\gamma(i) = \mathbf{H}_j(a,b)$, $i = i + 1$.
  End For
End For
End For.

As a result, the finger corresponding to the database that has the highest probability (3) becomes the signal source recognition result.

In the next section, we will describe the modified joint angle estimation method using this signal source recognition result.

5. **Modified Finger Joint Angle Estimation Method.** To solve the problem of our estimation method mentioned in Section 3, we propose a modified method using the signal source recognition result described in the previous section. In this method, we use the following equation instead of (1) to estimate the finger joint angle:

$$\theta(t) = \theta_0 + W\left\{\sum_{i=1}^{6} a_i X_i^f(t) + \sum_{j=1}^{6} b_j X_j^e(t)\right\} \tag{4}$$

where, a_i and b_i are weight coefficients and θ_0 is bias angle. These parameters can be obtained in a similar manner to (1). Moreover, the parameter W in (4) is a weight coefficient that reflects the activity of the subject finger and has a value between 0 and 1. If $W = 0$, it means that the estimated finger is inactive. Conversely, if $W = 1$, it means that the estimated finger is active. Therefore, using the value of W, we reflect the signal source recognition result in the finger joint angle estimation. In this paper, we calculate W using the least square method with respect to each motion of Table 1.

To confirm the effectiveness of the proposed method, we carried out the same finger joint angle estimation experiment as in Section 3. Here, we compared the proposed method with our previous estimation method using (1) as a conventional method. Figure 6 shows the joint angle estimation results for index finger and middle finger. In this figure, the solid line and dotted line denote the proposed method and the conventional method result, respectively. From Figure 6(a), it is found that both of the index finger (active finger) joint angle estimation results well converge to the measurement angle. As shown in Figure 6(b), the middle finger (inactive finger) joint angle estimation result of the proposed method is improved over that of the conventional method. This result indicates that our proposed method is effective for estimating 2 or more finger angles at same time.

Finally, we developed a myoelectric hand simulator that estimates the finger joint angle from surface EMG signals in real time using our proposed method. Figure 7 shows the myoelectric hand simulator and its estimation results. As shown, our simulator well

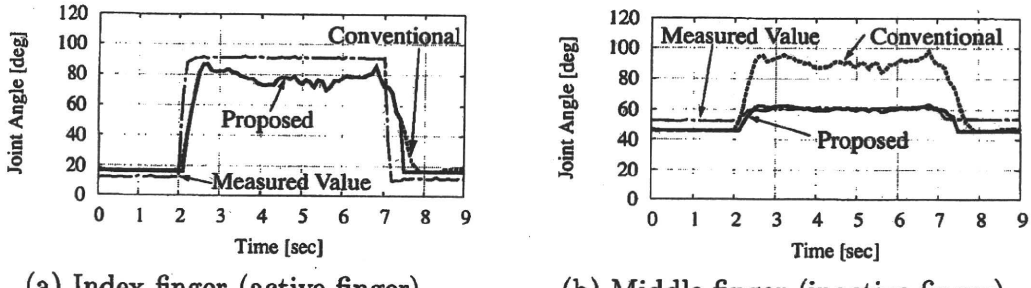

(a) Index finger (active finger) (b) Middle finger (inactive finger)

FIGURE 6. Estimation results of finger joint angle using proposed method and conventional method

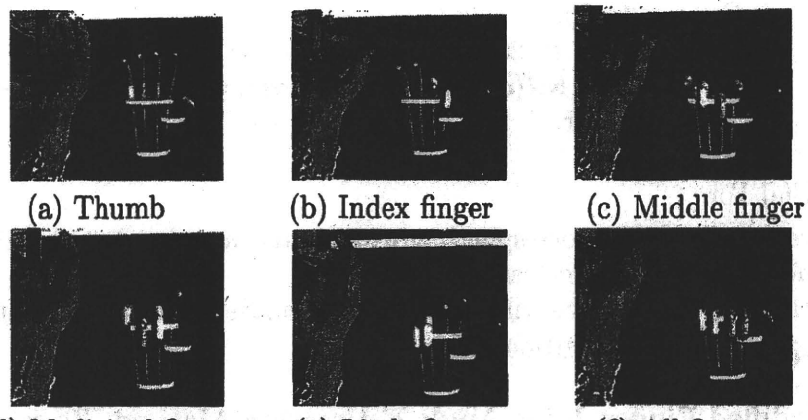

(a) Thumb (b) Index finger (c) Middle finger

(d) Medicinal finger (e) Little finger (f) All fingers

FIGURE 7. Motion of myoelectric hand simulator which implements our estimation algorithm

reproduces a user's hand motion from surface EMG signals. Our future work is to apply our proposed method to a real myoelectric hand.

6. **Conclusion.** This paper proposed a finger joint angle estimation method for a myoelectric hand using surface EMG signals and its source recognition results. The experimental results indicated that our proposed method is effective for estimating 2 or more finger angles at the same time. Moreover, we developed a myoelectric hand simulator by implementing our estimation algorithm and confirmed that our proposed method is technically feasible for application to a real myoelectric hand system.

REFERENCES

[1] H. Yokoi, W. Yu and K. Naruse, An autonomous adaptive control for the EMG prosthetic hand, *PO Academy Journal*, vol.10, no.1, pp.9-12, 2003.

[2] A. D. C. Chan and K. B. Englehart, Continuous myoelectric control for powered prostheses using hidden Markov models, *IEEE Trans. on Biomedical Engineering*, vol.52, no.1, pp.121-124, 2005.

[3] A. Katayama, S. Dok and Y. Koike, Estimation of finger posture with EMG signals for human interface, *Technical Report of IEICE*, vol.106, no.611, pp.7-12, 2007.

[4] Y. Yamamizu, N. Araki, Y. Konishi, K. Mabuchi and H. Ishigaki, Knuckle angle estimation method using histogram of surface EMG signals, *Proc. of the Symposium on Biological and Physiological Engineering*, vol.23, pp.183-184, 2008.

[5] N. Araki, Y. Konishi and H. Ishigaki, A statistical approach for handwritten character recognition using Bayesian filter, *International Journal of Innovative Computing, Information and Control*, vol.5, no.11(B), pp.4033-4040, 2009.

3-8-EP9

運動機能と感覚機能を備えた義手開発のための末梢神経再生型電極に関する研究 - 免疫組織学的検討

Immunohistrogical Evaluation of Regenerative Electrodes in Peripheral Nerves

[1]国立病院機構村山医療センター整形外科，[2]東京大学大学院情報理工学系研究科システム情報学専攻，[3]東京大学生産技術研究所マイクロメカトロニクス国際研究センター，[4]慶應義塾大学整形外科
○斎藤　治和[1]，満渕　邦彦[2]，鈴木　隆文[2]，
五條　理保[3]，池上　博泰[4]

【はじめに】近年，義手の情報ラインと神経系を直接インターフェイスデバイスで接続し，双方向のやりとりを行うことで，義手に運動及び感覚機能を付与する試みが行われている．このインターフェイス手法としては，中枢神経系に直接針電極を刺入する方法が現在主に試みられているが，刺入による中枢神経への損傷の可能性など安全性の問題がある．これに対し，末梢神経に装着する電極は安全性や信号の解釈が容易であるといった利点があるが，組織への固定性の問題がある．この問題を解決しうる電極として，切断した神経束の断端間に多数の電極孔の開いた電極をおき，孔を通過した再生軸索の活動電位を計測するという神経再生型電極が提唱されているが，その構造と神経再生についての詳細な研究は少ない．今回は孔の大きさを変えた神経再生型電極をラット坐骨神経に設置し，再生軸索の状態を免疫組織学的に検討したので報告を行う．

【材料および方法】ラット坐骨神経を大腿中央部で切断し，神経再生型電極を設置した．電極は孔の直径が20μ（20群），40μ（40群），60μ（60群），80μ（80群），100μ（100群）のものを用意した．2カ月後に電極を含む坐骨神経を取り出して固定後，凍結切片を作成し，抗ニューロフィラメント抗体および抗MBP（myelin basic protein）抗体による染色を行った．

【結果および考察】電極の遠位側の抗ニューロフィラメント抗体による染色では，20群は再生軸索が少なく，40以上の群では多数の再生軸索が認められた．抗MBP抗体による染色では，20群では陽性部分は小さく散在しており，40以上の群では比較的大きな陽性部分が多く見られた．これらから，40以上の群では，大径有髄線維も電極を通過して再生しているものと考えられた．

3-8-EP10

生体内におけるp38 MAPKを介した神経再生制御機構　第2報

Involvement of p38 MAPK in Regulatory Mechanism of Nerve Regeneration

[1]埼玉医科大学整形外科，[2]埼玉医科大学分子生物学講座，[3]三重大学医学部生化学講座
○加藤　直樹[1]，松本　征仁[2]，緒方　正人[3]，
禾　　泰壽[2]，織田　弘美[1]

セリン/スレオニンリン酸化酵素であるp38 MAPKは炎症の制御分子として，また，炎症治療の分子標的として注目されている．神経損傷後の炎症はWallerian変性とその後の神経再生において重要な意味をもつことから，これまで神経再生過程におけるp38の生理的機能について報告がなされてきた．しかしながらp38α遺伝子破壊マウスが胚性致死をきたすため，これらの報告はp38の阻害剤を投与することで検討されており，阻害剤の特異性の問題から相反する結果が導かれている．そこで我々はp38αの基質結合領域に点突然変異を導入したノックインマウス（semマウス）を作製し，p38のシグナル伝達を阻害することで，神経再生が組織学的にも機能的にも遅延すること，炎症性サイトカインであるTNFαの発現パターンに違いが生じることを見出し，昨年の本学会で報告した．

今回，こうした神経再生遅延の機序について，より詳細に検討する目的で，圧挫損傷後早期の再生軸索や軸索を取り囲むSchwann細胞，およびRhoAおよびMAGを抑制することで神経再生に促進的に作用するとされるIL-1βの発現などについて評価を行った．その結果，圧挫損傷部遠位の神経内に侵入する軸索の密度は，野生型と比較してsemマウスは有意差をもって低かった．また成熟Schwann細胞のマーカーであるS-100蛋白の発現，およびIL-1βの発現も野生型と比較してsemマウスで低下していた．

今回の個体レベルの解析結果から，semマウスにおける神経再生の遅延は，損傷後の軸索伸長の低下と，再生を支持するSchwann細胞の反応の違いにより生じていると思われた．神経再生において，p38 MAPK経路は単独で，他のシグナル伝達経路によって代償されない生理的機能を持つことが示され，p38 MAPK経路を明らかにすることで神経再生を制御できる可能性があると考えられた．

2-Pg-5

S100-GFP トランスジェニックラットを用いた骨格筋における神経筋接合部・神経分枝の形態学的検討 —速筋，遅筋での新たな形態的違いの発見—

加藤 征樹[1]　菊池 元史[2]　中間 季雄[3]　星野 雄一[1]
屋代 隆[2]

【目的】速筋の神経筋接合部は遅筋と比較しその構造がより複雑で大きく，さらに遅筋では神経終末の被覆の割合が多いとされ，その構造的差異は機能上の合目的な差と考えられる．筋タイプにより神経筋接合部の形態に違いがあるのであれば，神経分枝の走行パターンにも違いがあることが推測される．S100b のプロモーター下流に GFP 遺伝子を組み込んだ DNA を導入した S100-GFP トランスジェニックラット(Itakura et al. 2007) はシュワン細胞など S100b を発現している細胞の視覚化に有用である．本研究は，S100b-GFP トランスジェニックラットを用いてシュワン細胞を視認し，神経筋接合部と神経分枝に関して新たな観点から検討を行うことを目的とした．

【材料と方法】約 3 カ月齢の S100b-GFP ラット 5 匹を使用した．ヒラメ筋，総趾伸筋，前脛骨筋，腓腹筋内側・外側頭をそれぞれ取り出しホルマリン固定した．ショ糖処理を行い凍結ミクロトームを用いて切片を作成後，共焦点レーザー顕微鏡・蛍光顕微鏡で観察した．神経分枝の走行パターンは，フラクタル次元により評価・解析した．

【結果と考察】神経分枝の走行は速筋で有意にフラクタル次元が大きく，より緊密な構造を呈していた．最終分枝から神経筋接合部までの実測距離でも速筋がより短くかつ直線的に走行していた．速筋と遅筋では収縮速度やインパルスのパターンが異なることは合目的な違いと考えられているが，これを裏付ける結果が得られた．これは神経筋接合部も含め筋の収縮様式を達成するため形態的に適応した結果と考えられた．また遅筋の大多数の神経筋接合部において神経筋接合部の外周を城壁のように取り巻く S100 陽性細胞が確認されたが速筋では確認できなかった．近年，神経筋接合部での新たな細胞の存在が報告されているが，この細胞とは分布や形態が異なりかつ S100 陰性と報告されているので，全く別の細胞であると推測される．本細胞の詳細は不明だが，筋の収縮様式にも関与する神経筋接合部の細胞である可能性が推察され，現在検討中である．

【まとめ】速筋と遅筋では神経分枝の走行パターンが異なった．遅筋において神経筋接合部でこれまでに報告のない形態が確認された．

[1]自治医大整形外科　[2]自治医大解剖学教室　[3]下都賀総合病院整形

2-Pg-6

運動および感覚機能を備えた義手開発のための末梢神経再生型電極に関する研究 —至適電極孔径の検討—

斎藤 治和[1]　満渕 邦彦[2]　鈴木 隆文[2]　五條 理保[2]
池上 博泰[3]

【目的】近年，義手の情報ラインと神経系を直接インターフェイスデバイスで接続し，双方向のやりとりを行うことで，義手に運動および感覚機能を付与する試みが行われている．このインターフェイス手法としては，中枢神経系に直接針電極を刺入する方法が現在主に試みられているが，刺入による中枢神経への損傷の可能性など安全性の問題がある．これに対し，末梢神経に装着する電極は安全性や信号の解釈が容易であるといった利点があるが，組織への固定性の問題がある．この問題を解決しうる電極として，切断した神経束の断端間に多数の電極孔の開いた電極をおき，孔を通過した再生軸索の活動電位を計測するという神経再生型電極が提唱されているが，その構造と神経再生についての詳細な研究は少ない．今回は孔の大きさを変えた神経再生型電極をラット坐骨神経に設置し，再生軸索の状態を免疫組織学的に検討したので報告を行う．

【方法】ラット坐骨神経を大腿中央部で切断し，神経再生型電極を設置した．電極は孔の直径が 20 μ (20 群)，40 μ (40 群)，60 μ (60 群)，80 μ (80 群)，100 μ (100 群) のものを用意した．2 カ月後に電極を含む坐骨神経を取り出して固定後，凍結切片を作成し，抗ニューロフィラメント抗体および抗 MBP (Myelin Basic Protein) 抗体による染色を行った．

【結果】電極の遠位側の抗ニューロフィラメント抗体による染色では，20 群は再生軸索が少なく，40 以上の群では多数の再生軸索が認められた．抗 MBP 抗体による染色では，20 群では陽性部分は小さく散在しており，40 以上の群では比較的大きな陽性部分が多く見られた．

【考察および結論】末梢神経を構成する神経線維は，その伝導速度と径により分類がなされている．A 線維は小径および大径有髄線維であり，B 線維は有髄自律神経線維または節前線維，C 線維は小径無髄線維である．A 線維の直径は 2-12 μm，B 線維は 3 μm 未満，C 線維は 0.3-1.3 μm といわれている (Ganong1995)．抗ニューロフィラメント抗体染色による結果から，いずれの孔径の電極においても再生軸索が孔を通過して再生していることが示された．さらに，抗 MBP 抗体染色による結果から，孔の直径が 20 μm の場合は，A 線維の中でも比較的細い Aγ，Aδ 線維は通過している可能性はあるものの，太い Aα，Aβ 線維は通過できておらず，直径が 40 m 以上では，Aα，Aβ 線維も通過しているものと考えられた．

[1]国立病院機構村山医療センター整形外科　[2]東京大学大学院情報理工学系研究科システム情報学専攻　[3]慶應義塾大学整形外科

演題1：速順応型機械受容ユニットへの微小刺激により生成される振動感覚の周波数特性に関する基礎的研究

Basic study of spectral characteristics of vibration sensation evoked by microstimulation of rapidly adaptive mechanoreceptor units

抄録：触圧覚呈示機能を備えた義手を実現するための基礎的研究として、我々は機械受容ユニットへの微小電気刺激によって生成される感覚に関する研究を行っている。今回は、昨年度に引き続いて、速順応型機械受容ユニットを対象とした研究について報告する。実験ではまず正中神経へとタングステン微小針電極を経皮的に刺入し、速順応型機械受容ユニットを探索、同定した後に、生成される振動感覚の周波数を、反対側の手に実際に機械的振動刺激を加えて比較することにより求めた。結果としては微小電気刺激のパルス周波数と生成振動感覚の振動周波数は概ね一致するケースと、後者が前者の半分程度まで小さくなるケースとがあった。これらの結果、および機序に関する考察について報告する。

施設名：

1) 東京大学大学院情報理工学系研究科

2) 済生会横浜市東部病院 脳神経センター

1) Graduate School of Information Science and Technology, The University of Tokyo

2) Brain Nerve Center, Saiseikai Yokohama-city Tobu Hospital

演者名：

○鈴木隆文[1)], 矢口博彬[1)], 伊藤孝佑[1)], 満渕邦彦[1)], 國本雅也[2)]

○Takafumi Suzuki[1)], Hiroaki Yaguchi[1)], Kosuke Ito[1)], Kunihiko Mabuchi[1)], Masanari Kunimoto[2)]

連絡先：鈴木隆文

〒113-8656　東京都文京区本郷7−3−1、

東京大学 情報理工学系研究科 システム情報学専攻

電話番号：03-5841-6880、Fax 番号：03-5841-6882,

E-mail: t.suzuki@i.u-tokyo.ac.jp

演題２：SA-I mechano-receptive units の圧－発火特性に関する検討
－ preliminary study －

Classification of the SA-I mechano-receptor by the relationship between the applied pressure and the repetitive frequency of the generated spikes - a preliminary study -

抄録：我々は感覚機能を持つ義手の開発に関連して SA-I mechano-receptive unit に電気刺激のパルス列を加えて、人為的に任意の強度の圧感覚を発生させる研究を行なっている。その実験手順として、電気刺激を行なう前に、まず、マイクロニューログラム法によって、SA-I 機械受容器に与えた圧と unit に発生する発火頻度の関係を検討しているが、同じ SA-I unit でも圧－発火頻度特性は同じではなく、異なるサブグループが存在するという結果を得ており、現在、圧―発火頻度特性によって分類した場合、いくつのクラスタに分かれるか、についての検討を行なっている。まだ preliminary な段階ではあるが、これまで得られた結果について報告を行ない、このように複数の特性を示す受容器が存在する意義について考察を行なう。

施設名：
1. 東京大学情報理工学系研究科システム情報学専攻
2. 電気通信大学知能機械工学専攻
3. 済生会横浜市東部病院脳神経センター
1. Department of Information Physics and Computing, Graduate school of Information Science and Technology, The University of Tokyo
2. Department of Mechanical Engineering and Intelligent Systems, The University of Electro-Communications
3. Brain Nerve Center, Saiseikai Yokohamashi Tobu Hospital

演者名：
満渕邦彦[1]、新納弘崇[2]、國本雅也[3]、鈴木隆文[1]、矢口博彬[1]、下条 誠[2]、
Kunihiko Mabuchi[1], Hirotaka Niiro[2], Masanari Kunimoto[3], Takafumi Suzuki[1], Hiroaki Yaguchi[1], Makoto Shimojo[2]

連絡先：満渕邦彦（corresponding author）
〒113-8656　東京都文京区本郷 7－3－1、
東京大学 情報理工学系研究科 システム情報学専攻
電話番号：03-5841-6880、Fax 番号：03-5841-6882,
E-mail: Kunihiko_Mabuchi@ipc.i.u-tokyo.ac.jp

演題３：末梢神経障害による感覚障害に対するマイクロスティミュレーション法を用いた感覚補填・感覚強化システムモデルの構築

A model of the sensory prosthetic and enhancement system for sensory disturbances due to peripheral neural disorders using micro-stimulation method

抄録：末梢神経傷害による感覚機能障害に対して、マイクロスティミュレーション法を用いて感覚機能の補填・強化を行なうシステムのモデルの構築を行なった。まず、正中神経にマイクロニューログラム針電極を刺入して SA-I single unit に当てる。次に、その投射野の指に、外部からの圧刺激が直接指の圧受容器に影響しない様に硬いプラスチックの指サックを被せる。さらにその上に圧センサを装着してこれをバーで押し、検出された圧を電気刺激パルス列に変換し、マイクロスティミュレーション法を用いて unit の電気刺激を行ない、圧感覚を発生させた。その結果、検出した圧を電気刺激パルス列の繰り返し頻度に変換する係数を調節する事により、加えた圧と同じ強度の圧感覚を発生させる事が出来、又、弱い圧を強い圧として強化・提示する事も可能である事を示した。なお、電気刺激により発生する圧の強さの評価は、被験者が反対の手で圧センサを押し込み提示するという方法を用いた。

施設名：

1. 電気通信大学知能機械工学専攻
2. 済生会横浜市東部病院脳神経センター
3. 東京大学情報理工学系研究科システム情報学専攻

1. Department of Mechanical Engineering and Intelligent Systems, The University of Electro-Communications
2. Brain Nerve Center, Saiseikai Yokohamashi Tobu Hospital
3. Department of Information Physics and Computing, Graduate school of Information Science and Technology, The University of Tokyo

演者名：

新納弘崇[1]、下条 誠[1]、國本雅也[2]、鈴木隆文[3]、石川正俊[3]、矢口博彬[3]、満渕邦彦[3]

Hirotaka Niiro[1], Makoto Shimojo[1], Masanari Kunimoto[2], Takafumi Suzuki[3], Masatoshi Ishikawa[3], Hiroaki Yaguchi[3], Kunihiko Mabuchi[3]

連絡先：満渕邦彦（corresponding author）

〒113-8656　東京都文京区本郷 7－3－1、

東京大学 情報理工学系研究科 システム情報学専攻

電話番号：03-5841-6880、Fax 番号：03-5841-6882,

E-mail: Kunihiko_Mabuchi@ipc.i.u-tokyo.ac.jp

感覚神経系障害患者のための
ウェアラブル感覚補填・感覚強化システムの開発
～マイクロスティミュレーション法による触圧覚生成と感覚増強～

Wearable sensory prosthetic system for patients with sensory disturbance
-generation of somatic sensation and its enhancement using microstimulation method-

○新納 弘崇 (電通大)　國本 雅也 (済生会横浜市東部病院)　鈴木 隆文 (東京大)　満渕 邦彦 (東京大)　下条 誠 (電通大)

Hirotaka Niiro(UEC),Masanari Kunimoto(Saiseikai Hosp.),Takafumi Suzuki(Univ. of Tokyo),
Kunihiko Mabuchi(Univ. of Tokyo),Makoto Shimojo(UEC)

Abstract— In this study, we attempted to develop a prototype of a wearable sensory prosthetic system with which patients suffering from peripheral sensory disturbance will be able to feel somatic sensations as if they were touching an object with their healthy and intact hand. The system consists of finger sacs and palm patch equipped with flexible pressure sensors, and micro-electrical stimulation of the sensory nerve fibers was used in order to evoke somatic sensations. The results showed that the system worked satisfactorily, and it is demonstrated that the system will be able to compensate or even enhance sensory function of the patients with sensory neuropathy.

Key Words: sensory feedback,intelligent prosthetic hand,work support,microstimulation method

1. 緒言

病気や事故によって感覚を失ってしまった場合，日常生活に多大な支障をきたす事になる．そこで，障害によって失った感覚を回復するための一つの方法として，感覚神経電気刺激を利用した感覚を提示する研究がなされるようになった [1].

実際の生体では，感覚受容器が受けた刺激を活動電位のパルス列に変換し，中枢に伝達されることで感覚を得る [2]．そして，刺激を伝える感覚神経線維に同じ活動電位列を発生させることができれば，実際に刺激を受けた時と同じ感覚を得ることができる．

そこで本研究では，触覚センサの情報をマイクロスティミュレーション法を用いて，感覚神経経由により触感覚として提示するシステムの開発を目的とした．

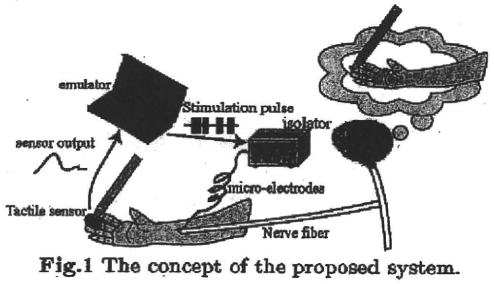

Fig.1 The concept of the proposed system.

2. 実験システム

実験システムの全体構成を図 2 に示す．システムは触覚センシングと神経線維インターフェースの 2 つに分かれている．前者は被験者の指先に装着した触覚センサの情報をコンピュータに取り込み，後者は取り込んだ情報に応じて神経線維を刺激するパルス列を出力する．以下各実験システムについて説明する．

2.1 触覚センサ

触覚センサとして FingerTPS(PPS 社製) を用いた．センサは人の手に装着し，接触力を検出するフレキシブルな静電容量型圧力センサである．出力は Bluetooth 通信で PC に接続され，40Hz で更新する．

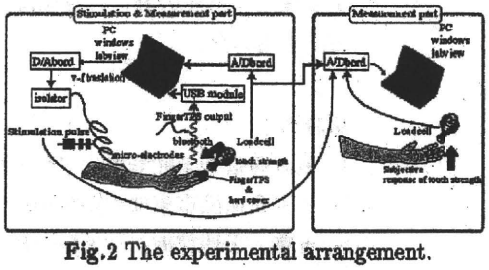

Fig.2 The experimental arrangement.

2.2 神経線維インターフェース

触覚センサからの情報を基にマイクロスティミュレーション法を用いて感覚を被験者に提示する．マイクロスティミュレーション法とは，経皮的に微小針電極を感覚神経線維の中に刺入し，電気刺激パルス列を入力することで，人工感覚を生成する手法である．

Fig.3 The Finger TPS system.

Fig.4 The manner in which microstimulation is performed.

3. 感覚提示実験

感覚神経への電気刺激によって生成される圧感覚の強度はパルス頻度に依存している [3] 事が報告されており，本研究ではこの関係を応用する．

3.1 実験目的・方法

本実験の被験者は，健全な男性 1 名である．被験者は座っており，開眼状態で実験を行った．指先に加えた力によって発生する感覚と等価な感覚量を感覚神経の電気刺激で発生させることを目的とする．この為には，指先に発生した感覚を定量評価する必要がある．今回我々は生成された感覚の計測法として，加圧した指先に発生される力と反対の指先でその力に対し等価な感覚量を提示させることとした．

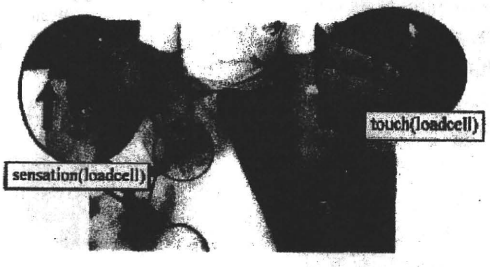

Fig.5 Quantitative evaluation of the pressure sensation evoked by microelectricqal stimulation.

3.2 機械刺激に対する感覚量

まず，片方の指先に力を加え，その力と同等の力を反対の指先で提示する実験を行った．実験結果を図 6 に示す．加圧力と感覚量の相関係数は 0.98 であり，相関が高いことから，皮膚表面に加えた機械刺激と感覚量の関係はほぼ等価な関係であることが示された．

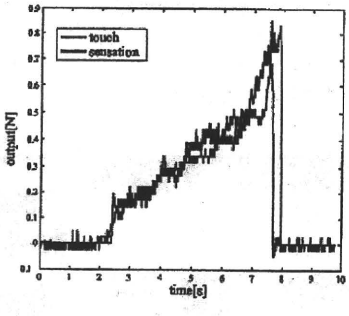

Fig.6 Actual force applied to the TPS sensor and the subjective magnitude of the evoked pressure sensation.

3.3 電気刺激に対する感覚量

次に，指先にハードカバーを装着し，感覚を遮断した状態で感覚を提示する実験を行った．FingerTPS の出力をパルス列頻度に変換・出力し，マイクロスティミュレーション法によりパルス列を神経に伝達することで感覚を提示した (図 7)．

本実験では，圧覚から電気刺激のパルス列頻度への変換式は，FingerTPS の出力 x を係数 a にて整数倍し，これをパルス頻度の周波数 f とした．即ち，$f = ax$ で，本実験では $a = 50$ とした．

Fig.7 The manner in which a subject enhances somatic sensations by the developed system.

実験結果の一例を図 8 に示す．グラフは上から FingerTPS と加圧力と感覚量，出力周波数，出力パルスである．実験結果をみると，パルス頻度が増加することによって被験者の感覚量は増加している．押付力と感覚量の関係は相関係数 0.91 であり，高い相関があることから被験者の感覚を生成出来ていることがわかる．また，FingerTPS と押付力との相関係数は 0.97 であり，FingerTPS が接触力を忠実に再現出来ていることが確認できる．

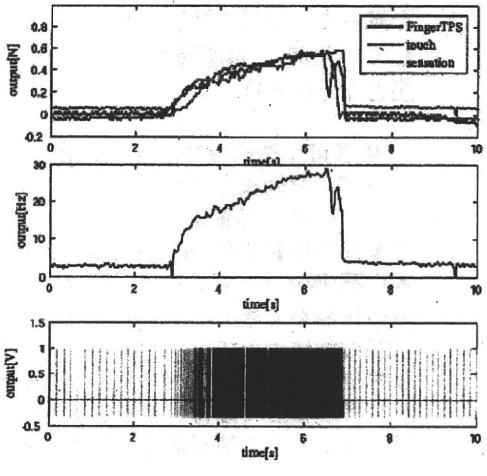

Fig.8 Response of subjective pressure sensation evoked by the microelectrical stimulation, pulse train for the microelectrical stimulation, and the actual force applied to the Finger TPS system,

4. 結言

触覚センサの出力をマイクロスティミュレーション法により神経フィードバックし，人工感覚を提示するシステムを構築した．触覚センサの出力をパルス変換し，マイクロスティミュレーション法により提示することで失われた感覚を補綴しうる可能性を示した．

文 献

[1] M.Shimojo,T.Suzuki,A.Namiki,T.Saito,M.Kunimoto, R.Makino,H.Ogawa,M.Ishikawa,K.Mabuchi "Development of a system for experiencing tactile sensation from a robot hand by electrically stimulating sensory nerve fiber" IEEE Trans.Robotics and Automation(CD-ROM),2003

[2] Kandel,Schwartz,Jessell"PRINCIPLES OF NUERAL SCIENCE Fourth Edition",McGraw-Hill,2000

[3] T.Suzuki,K.Mabuchi,H.Nishimura,T.Saito,N.Kakuta, M.Kunimoto,M.Shimojo,The Relationship between Stimulation Signals and Subjective Intensities and Areas, Proc. Int. Conf. of the IEEE EMBS,Atlanta, 459, Oct. 1999.

多層配線構造を有する神経再生型電極の開発

○吉田 充宏[1]、浮田 芳昭[1]、満渕 邦彦[2]、内海 裕一[1]
1. 兵庫県立大学高度産業科学技術研究所、2. 東京大学大学院情報理工学系研究科

1. はじめに

神経再生型電極は、末梢神経の再生現象を利用した方法であり、臨床の場ではおもに義肢等のインターフェイスとしての利用を目的とされている。原理としては、一旦切断した神経束の近位端と遠位端を、中隔を挟んで対向する形で位置させると、切断された神経軸索が近位側から再生し、電極孔を通過して末梢側に伸長して行く。これにより電極と軸策とが物理的かつ電気的に強固に固定され、電極孔を通過した再生軸索の活動測定と電気刺激が孔に設置した電極で行えるようになる。

2. 多チャンネル化可能な電極の設計

今回の設計・試作において、電極孔の大きさは神経線維の径の個体差も考慮した上で 30、60、90μm の 3 種類の大きさで、個々の電極が計測時に干渉しないように電極部の配線、配線間の幅は最小の部分で 20μm、電極部の金層の厚み 12μm と設定した。また、多チャンネル化を行うにあたり、単層での電極層では配線の密度などからチャンネル数に限界が生じる。そのため、本研究では電極層を積層させ、三次元構造とすることでの作製を試みた。積層させることで、1 層あたりでは電極を 12 個配置していたが、2 層積層することで計 24 個の電極の配置が実現可能となる(Fig.1)。

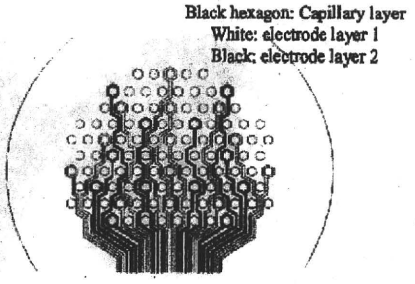

Fig.1 積層構造の電極部

3. 神経再生型電極の作製プロセス

まず、黄銅板上にレジスト AZP4903(AZ エレクトロニクスマテリアルズ(株))を用いてフォトリソグラフィにより電極部のパターニングを行い(Fig.2-a)、パターニングした部分に Au メッキをすることで電極部の作製を行い(Fig.2-b)、AZP4903 を除去することで電極部を自立させる(Fig.2-c)。そして、SU-8(日本化薬(株))のフォトリソグラフィにより絶縁層を作製し(Fig.2-d)、黄銅板を除去することで単層の電極層の作製ができる(Fig.2-e)。積層を行うため、この作業を 2 種類の電極のパターン①、②で行う。次に、積層方法については、パターン①の電極層を SiO_2 基板の上に置き(Fig.2-e)、中間の絶縁層となる SU-8 を塗布し(Fig.2-f)、パターン②の電極層とアライメントを行う(Fig.2-g)。そして、圧力をかけながら加熱を行うことで接合させる(Fig.2-h)。その後、中間層のフォトリソグラフィによりキャピラリー部を貫通させることで積層構造を有する神経再生型電極の作製ができる(Fig.2-i)。

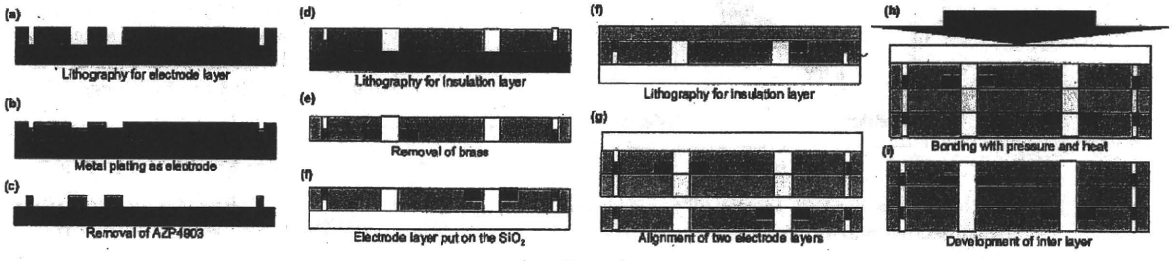

Fig.2 全工程のプロセスフロー

4. まとめ

今回作製した電極の写真を Fig.3 に示す。本研究では、神経再生型電極の多チャンネル化を実現させるため、電極層を 2 層積層することにより三次元的に作製する方法の検証を行い、それが可能であることを初めて実証した。今後は、構造パラメータの最適化と積層段の多段化、並びに作製プロセスの高度化を目指す。また、実装による実際の神経信号の計測等による検証も行っていく必要がある。

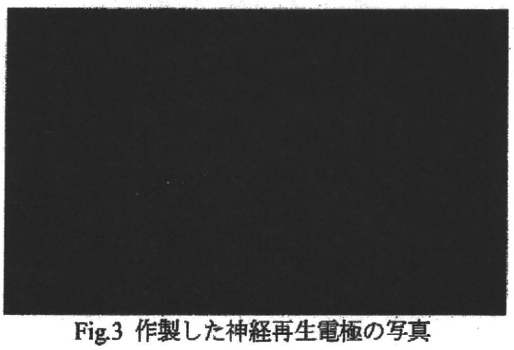

Fig.3 作製した神経再生電極の写真

Proposal of stacked electrodes for multiplex neural interface

Mitsuhiro Yoshida[1], Yoshito Hirose[1], Yoshiaki Ukita[1], Kunihiko Mabuchi[2], Yuichi Utsumi[1]
[1]Laboratory of Advanced Science and Technology for Industry, University of Hyogo,
3-1-2 Koto, Kamigori, Ako-gun, Hyogo, 678-1205, Japan
[2]Graduate School of Information Science and Technology, The University of Tokyo,
7-1-3, Hongo, Bunkyo-ku, Tokyo, 113-8656, Japan
Phone: +81-791-58-0232, Fax: +81-791-58-0232, E-mail: mituhiro@lasti.u-hyogo.ac.jp

Information on the nervous system is expressed by the trains of action potentials transmitted through the axons from neurons and this neural signal can be detected by mounting electrodes close to the nerve fibers or nerve cells. Also, nerve signals can be generated by stimulating the nerve cells or nerve fibers [1]. Recently such technology has become widely used not only for brain machine interface (BMI) systems in clinical medicine but also for investigating nervous functions in the field of basic neural sciences. In such fields, in addition to analyzing nerve signals of a single neuron or single axon, it is also very important to analyze neural information expressed by network-level in the nervous system. Key to doing this is developing neural electrodes that can record and/or stimulate neurons or axons simultaneously with many channels. Thus, a nerve regeneration electrode system is proposed as a candidate for such electrodes [2]. This electrode is designed for recording signals of peripheral nervous system and uses peripheral nerve regeneration. The concept of the electrode is as follows (see Fig.1). We cut a peripheral nerve trunk once and face the proximal stump and distal stump towards each other in a guide tube for regeneration. At this time, between the two stumps we put a septum with many holes that all electrode sites. Then cut axons begin to regenerate and extend from the proximal side, pass through the electrode holes of the septum, and it has thus become possible to measure the electrical activity of the axons or simulate them electrically by using the electrode holes.

A very serious problems with the nerve regeneration electrode is wiring from/to the electrode sites. The nerve regeneration electrode must be equipped with a huge number of electrode channels, which means that the wiring to and from the electrode holes has inevitably become very complex. In this study, we designed and manufactured a regeneration electrode with which we can solve the upper-mentioned wiring problem by using the stacked structure of the electrodes. Figure 2 (a) outlines the schematic diagram of the nerve regeneration electrode. To increase the number of electrodes we propose a stacked electrode structure. It is difficult to integrate many electrodes by using single layer due to the restriction of the integration of each electrode area. Thus the electrode shape is designed to be stacked, enabling three-dimensional (3D) inter connection of multiple electrode lines. The first attempt achieved two designed electrode structures with 12 channels stacked on a substrate and total 24 channels. Figure 2 (b) shows the designed nerve reproduction electrodes.

The proposed stacked electrodes were fabricated on the basis of multiple stacking SU-8-layers [3]. The prepared single layer electrode chips were piled up together by using precise alignment and bonding processes. Figure 3 shows the fabrication process image of bonding. To bond the electrodes without bounding reagent, the unique characteristic of SU-8 is utilized for the patterning of capillaries and bonding. The SU-8 was exposed to UV light to pattern the through hole structure, achieving stronger bonding between two bonded surfaces. Figure 4 (a) shows the outer view of fabricated electrodes. Figure 4 (b) zooms in on the structure of electrodes. As shown in Fig.4 (b), the three-dimensionally stacked electrodes and through capillary for nerve growth are successfully aligned and patterned in monolithic SU-8 chip. We developed the method to manufacture a three-dimensional electrodes structure to realize the multi channel for the flexible-regeneration nerve electrode. The structure parameter and the stacking step of the fabrication process need to be further optimized evaluated by adapting it to the measurement of an actual neural coding with mounting on animals.

REFERENCES

[1] Å. B. Vallbo, K. E. Hagbarth, and B. G. Wallin, J Apply Physiol, Vol. 96, pp.1262-1269 (2004)
[2] T. Suzuki, T. Saito and K. Mabuchi, Technical report of IEICE, Vol. 100, No. 479 pp.63-66 (2000)
[3] F. J. Blanco, M. Agirregabiria, J. Garcia, J. Berganzo, M. Tijero, M. T. Arroyo, I. Aramburu and K. Mayora, J.Micromech. Microeng, Vol. 14, pp.1047-1056 (2004)

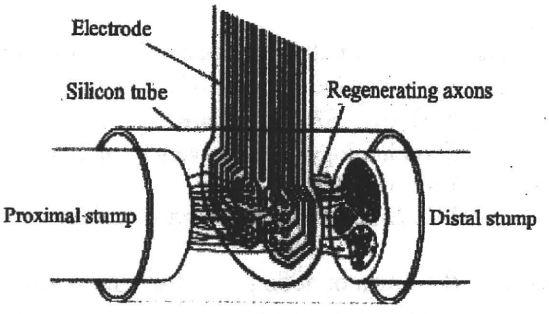

Fig.1 Model of nerve regeneration electrode

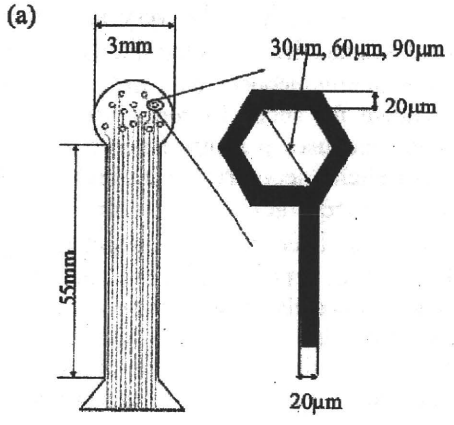

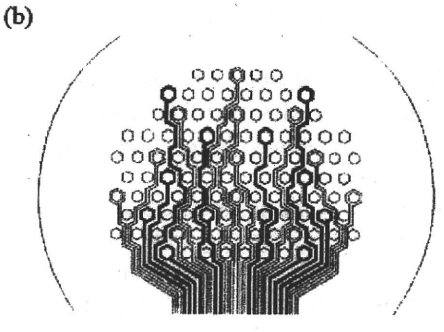

Black hexagon: capillary layer
White: electrode layer 1
Black: electrode layer 2

Fig.2 (a) Outline of electrode
(b) Designed nerve regeneration electrodes

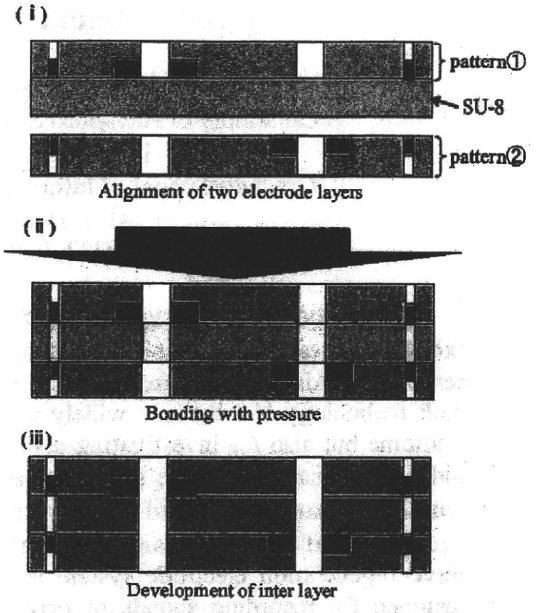

Fig.3 Fabrication process image of bonding

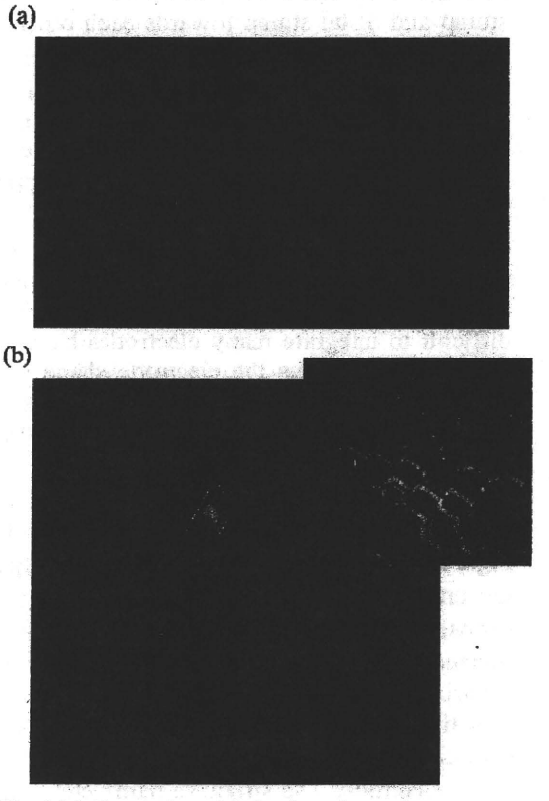

Fig.4 (a) Outer view fabrication electrodes
(b) Zoom in on structure of electrodes

Phase-Compensated Averaging for Analyzing Electroencephalography and Magnetoencephalography Epochs

Ayumu Matani*, *Member, IEEE*, Yasushi Naruse, Yasushi Terazono, Taro Iwasaki, Norio Fujimaki, *Member, IEEE*, and Tsutomu Murata

***Abstract*—Stimulus-locked averaging for electroencephalography and/or megnetoencephalography (EEG/MEG) epochs cancels out ongoing spontaneous activities by treating them as noise. However, such spontaneous activities are the object of interest for EEG/MEG researchers who study phase-related phenomena, e.g., long-distance synchronization, phase-reset, and event-related synchronization/desynchronization (ERD/ERS). We propose a complex-weighted averaging method, called phase-compensated averaging, to investigate phase-related phenomena. In this method, any EEG/MEG channel is used as a trigger for averaging by setting the instantaneous phases at the trigger timings to 0 so that cross-channel averages are obtained. First, we evaluated the fundamental characteristics of this method by performing simulations. The results showed that this method could selectively average ongoing spontaneous activity phase-locked in each channel; that is, it evaluates the directional phase-synchronizing relationship between channels. We then analyzed flash evoked potentials. This method clarified the directional phase-synchronizing relationship from the frontal to occipital channels and recovered another piece of information, perhaps regarding the sequence of experiments, which is lost when using only conventional averaging. This method can also be used to reconstruct EEG/MEG time series to visualize long-distance synchronization and phase-reset directly, and on the basis of the potentials, ERS/ERD can be explained as a side effect of phase-reset.**

***Index Terms*—Alpha rhythm, alpha ringing, averaging, electroencephalography (EEG), event-related synchronization/desynchronization (ERS/ERD), long-distance synchronization, megnetoencephalography (MEG), phase-reset.**

Manuscript received July 17, 2009; revised October 9, 2009 and November 27, 2009. First published February 17, 2010; current version published April 21, 2010. This work was supported in part by a grant-in-aid for scientific research (B) from the Ministry of Education, Science, Sports and Culture under Grant 21300102. *Asterisk indicates corresponding author.*

*A. Matani is with the Graduate School of Frontier Sciences, the University of Tokyo, Kashiwa 277-8561, Japan, and also with the Biological ICT Group, National Institute of Information and Communication Laboratory, Kobe 651-2492, Japan (e-mail: matani@isp.ac).

Y. Naruse and T. Murata are with the Biological ICT Group, National Institute of Information and Communication Laboratory, Kobe 651-2492, Japan.

Y. Terazono and T. Iwasaki are with Graduate School of Frontier Sciences, the University of Tokyo, Kashiwa 277-8561, Japan.

N. Fujimaki is with the Biological ICT Group, National Institute of Information and Communication Laboratory, Kobe 651-2492, Japan, with Graduate School of Life Science and Systems Engineering, Kyushu Institute of Technology, Kitakyushu 808-0196, Japan, and also with the Human Information System Laboratories, Kanazawa Institute of Technology, Kanazawa, Ishikawa 921-8501, Japan.

Color versions of one or more of the figures in this paper are available online at http://ieeexplore.ieee.org.

Digital Object Identifier 10.1109/TBME.2009.2038363

I. Introduction

STIMULUS-LOCKED averaging (conventional averaging, hereafter) is often used for analyzing electroencephalography (EEG) and magnetoencephalography (MEG) epochs to enhance the signal-to-noise ratio (SNR). However, EEG and MEG (xEG, hereafter) researchers differ in their concepts of signal and noise. Spontaneous activities, which are observed as rhythmic activities in each epoch, are canceled out by conventional averaging, since they are not stimulus-locked. The mean xEG time series, or the stimulus-evoked activity in the narrow sense, is considered to be the signal, and ongoing spontaneous activities are considered to be noise.

On the contrary, xEG researchers who study phase-related phenomena, e.g., long-distance synchronization, phase-reset, and event-related synchronization/desynchronization (ERS/ERD), are rather interested in ongoing spontaneous activities. Some xEG researchers think that the mean time series is not stimulus-evoked but stimulus-induced via a phase-reset of ongoing spontaneous activity [1], and there is a relationship between phase-reset and alpha ringing, which is the alpha-band synchronization appearing around 0.5–0.9 s after stimulus onset [2]. Some xEG researchers believe that ERS/ERD of ongoing spontaneous activity plays a functional role [3]. Some xEG researchers are interested in the rhythmic synchronization between distant brain areas, called long-distance synchronization [4]. The amount of synchronization has been evaluated by using an index called the phase-locking value (PLV). Recently, the directional relationship between two brain areas has been investigated via phase synchronization [5]. The directional relationship has been quantitatively evaluated by using an index, called the Granger causality spectra, based on a multivariate autoregressive model. The ongoing spontaneous activities are considered to be signals, and therefore, conventional averaging is not appropriate for their analyses.

Can the ongoing spontaneous activities be averaged instead of averaging the stimulus-evoked activity? Also, can the directional relationship of ongoing spontaneous activities between xEG channels be evaluated as an xEG time series not instead of as an index? If such an xEG time series can be obtained, conventional analyses for processing xEG time series (e.g., solving xEG inverse problem) can be applied to it.

In this paper, we propose an extended stimulus-locked averaging method, called phase-compensated averaging. This method

seeks to average an ongoing spontaneous rhythm and to evaluate the directional phase-synchronizing relationship between xEG channels by setting any xEG channel as a trigger channel.

II. Method

A. Concept of Phase-Compensated Averaging

External triggering for conventional averaging is usually performed by using a time series generated by an external device for stimulation. The trigger timings are determined by the characteristics of the time series. The timings at which the amplitude exceeds a specific threshold value will be the trigger timings. Therefore, a pulse train, which has no essential meaning for stimulation, is often employed as the time series for triggering.

On the other hand, internal triggering is often used for averaging electrocardiography (ECG) and/or magnetocardiography (MCG) epochs. The trigger timings are determined by the characteristics of a single ECG/MCG (xCG, hereafter) epoch. For instance, the timings at which the amplitude of QRS complexes reach individual peaks can be used as the trigger timings.

In external and internal triggering, trigger timings are determined by the amplitude characteristics of the time series. Assuming that the time series is complex-valued, phase characteristics can alternatively be used. For instance, the timings at which the phase of the time series reaches a specific value can be used as the trigger timings.

Unfortunately, a single xEG epoch does not have conspicuous amplitude characteristics like those of single xCG epoch. Therefore, to find reliable trigger timings, internal triggering based on amplitude is not appropriate, and we may be forced to use external triggering based on amplitude. However, internal triggering based on phase can be associated with external triggering based on amplitude; i.e., xEG epochs can be compensated such that their instantaneous phases at the external trigger timings are set to a specific value. This phase compensation is worth considering at least for the following reason. Conventional averaging cancels out ongoing spontaneous activities on the basis of the fact that the instantaneous phases of epochs at the external trigger timings are uniformly distributed. If these phases are compensated to lock in a specific value, ongoing spontaneous activities should appear with a high SNR after averaging.

B. Procedure of Phase-Compensated Averaging

Fig. 1 shows a schematic diagram of phase-compensated averaging. Preprocessing [see Fig. 1(a)] is done prior to averaging [see Fig. 1(b)].

In Fig. 1(a), the xEG time series of the lth channel, qth epoch ($q = 0,1,\ldots,Q-1$), and nth time sampling point is denoted by $x_{lq}[n]$ ($n = 0$ is the external trigger timing). First, $x_{lq}[n]$ is narrow-band filtered to get $x^{\mathrm{N}}_{lq}[n]$. The passband is selectable. For instance, if xEG researchers are interested in the alpha-band phase modulation, the frequency from the alpha to beta band, taking the frequency shift by the phase modulation into account, would be the best choice. Second, $x^{\mathrm{N}}_{lq}[n]$ is discrete Hilbert transformed [7] to get $\tilde{x}^{\mathrm{N}}_{lq}[n]$, which is a complex-valued xEG of $x^{\mathrm{N}}_{lq}[n]$, and the instantaneous phase is simply determined as

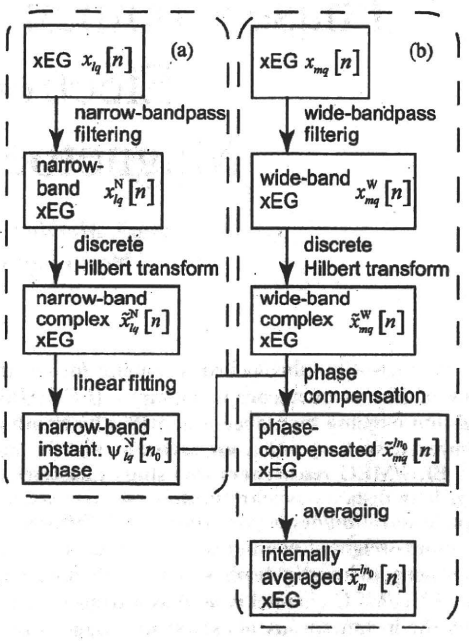

Fig. 1. Schematic diagram of phase-compensated averaging. (a) Instantaneous phase of the narrow-band xEG of the lth channel and the qth epoch at the n_0th time sampling point $\psi^{\mathrm{N}}_{lq}[n_0]$ is calculated. (b) Average of the wide-band xEG of the mth channel compensated by $\psi^{\mathrm{N}}_{lq}[n_0]$, $\bar{x}^{ln_0}_{m}[n]$, is calculated.

$\mathrm{Arg}\{\tilde{x}^{\mathrm{N}}_{lq}[n]\}$. Since the discrete Hilbert transform (DHT) is actually zero-padding in the frequency domain, narrow-bandpass filtering can be involved in DHT by padding additional zeros to the stopband. Finally, the instantaneous phase at time sampling point n_0, $\psi^{\mathrm{N}}_{lq}[n_0]$, is precisely calculated by using a least squares fit of the first-order polynomial to the instantaneous phase in duration G, $\mathrm{Arg}\{\tilde{x}^{\mathrm{N}}_{lq}[n]\}_{n\in G}$, where n_0 is the center time sampling point in G and will be the trigger timing. G is set to one period of the frequency band of interest to fit the narrow-band, e.g., 0.1 s for fitting to the alpha band. Note that the only production in the series of procedures in Fig. 1(a) is $\psi^{\mathrm{N}}_{lq}[n_0]$, and hence $\tilde{x}^{\mathrm{N}}_{lq}[n]$ is no longer used.

In Fig. 1(b), the procedure for obtaining a wide-band complex-valued xEG $\tilde{x}^{\mathrm{W}}_{mq}[n]$ of the mth channel is the same as in Fig. 1(a), except for the passband. This passband is set to the one that xEG researchers usually select, and hence, it is relatively wide-band. $\tilde{x}^{\mathrm{W}}_{mq}[n]$ is phase-compensated by $\psi^{\mathrm{N}}_{lq}[n_0]$ as

$$\tilde{x}^{ln_0}_{mq}[n] = \tilde{x}^{\mathrm{W}}_{mq}[n]\exp\left(-\mathrm{j}\psi^{\mathrm{N}}_{lq}[n_0]\right) \tag{1}$$

where j is the imaginary unit. The phase compensation (1) indicates that the mth channel xEG is compensated such that the instantaneous narrow-band phase of the lth channel is 0 at n_0. Since $\tilde{x}^{\mathrm{W}}_{mq}[n]$ is complex-valued, this compensation is actually a rotation on the complex plane. Finally, we obtain the average of the mth channel compensated by the lth channel as

$$\bar{x}^{ln_0}_{m}[n] = \frac{1}{Q}\sum_{q=0}^{Q-1}\tilde{x}^{ln_0}_{mq}[n]. \tag{2}$$

The DHT for determining the narrow-band instantaneous phase $\psi_{lq}^{\mathrm{N}}[n_0]$ [see Fig. 1(a)] can be replaced with a wavelet-based method [2], [4]. The difference between the results of these two methods is minor [9]. However, a sort of integration of the phases in the narrow-band is necessary for a wavelet-based method to determine a representative phase. The reason for employing DHT is that it involves such an integration. The aforementioned procedure of phase-compensated averaging was implemented in MATLAB.

C. Auto and Cross Averages

Phase-compensated averaging embodies a new concept, auto and cross averages. We call the case of $l = m$ in averaging (2) auto average and the case of $l \neq m$ cross average. In phase-compensated averaging, any xEG channel can be used for internal triggering, so there is no need to distinguish internal and external channels. Accordingly, the conventional average is a cross average compensated by the external trigger channel.

We would like to emphasize that cross averaging is directional, namely $\bar{x}_m^{ln_0}[n] \neq \bar{x}_l^{mn_0}[n]$. Therefore, phase-compensated averaging can selectively average ongoing spontaneous activity phase-locked in any xEG channel. In other words, phase-compensated averaging can evaluate the directional relationship of ongoing spontaneous activities between xEG channels as xEG time series.

D. Another Interpretation

The phase-compensated average is approximated by the first term of the discrete Fourier transform of over sorted epochs as follows. Since stimuli are repeatedly presented with random timings, instantaneous phases are uniformly distributed from 0 to 2π in the case that n_0 is chosen at a pretrigger time sampling point. Now, let $\eta[q]$ be the epoch order permutation function that sorts the epochs in ascending order of $\psi_{lq}^{\mathrm{N}}[n_0]$ from 0 to 2π. We have the following approximation:

$$\psi_{l\eta[q]}^{\mathrm{N}}[n_0] \simeq \frac{2\pi q}{Q}. \tag{3}$$

Substituting approximation (3) into the phase-compensated average (1) and (2), we obtain an interpretation of this averaging with the first term of the discrete Fourier transform

$$\bar{x}_m^{ln_0}[n] \simeq \frac{1}{Q}\sum_{q=0}^{Q-1} \tilde{x}_{m\eta[q]}^{\mathrm{W}}[n] \exp\left(-\mathrm{j}\frac{2\pi lq}{Q}\right). \tag{4}$$

Fourier form (4) immediately leads to the interpretation that the conventional average corresponds to the zeroth term of the discrete Fourier transform. Phase-compensated averaging is an extension of conventional averaging.

This Fourier interpretation introduces the concept of signal and noise. The power of epochs in the time domain is distributed over the epochs in the frequency domain in the sense of Parseval's theorem. While using only conventional averaging treats the first and higher terms as noise, simultaneous use of conventional and phase-compensated averaging treats the second and higher terms as noise. This means information that would otherwise be lost by performing only conventional averaging can be recovered by using phase-compensated averaging.

III. Simulation I: Fundamental Characteristics

A simulation was performed to reveal the fundamental characteristics of phase-compensated averaging.

A. Given Epochs

Two-channel ($m = 1, 2$) and 200-trial ($q = 0, 1, \ldots, 199$) xEG epochs $x_{mq}(t)$, $(-0.2 \leq t \leq 0.5\,\mathrm{s})$, were given as

$$x_{mq}(t) = x^{\mathrm{EV}}(t) + x_{mq}^{\alpha}(t) + R_{mqt}^{\mathrm{N}}(0, 0.3) \tag{5}$$

where

$$x^{\mathrm{EV}}(t) = \exp(-5 \times 10^3 (t - 0.1)^2) + 0.5\exp(-10^3 (t - 0.2)^2) \tag{6}$$

is the common stimulus-evoked activity, $x_{mq}^{\alpha}(t)$ is alpha-band activity having trial-wise different initial phases, and $R^{\mathrm{N}}(a, b)$ is additive noise in the form of normally distributed random numbers with mean a and standard deviation b with respect to each of the subscripts (m, q, and t).

Let us explain $x_{mq}^{\alpha}(t)$ in detail. $x_{mq}^{\alpha}(t)$ includes directional phase modulation from channel 1 to channel 2 as follows. First, the phases of $x_{mq}^{\alpha}(t)$ are prepared as

$$\theta_{1q}(t) = \psi_{1q}(t)$$

$$\theta_{2q}(t) = \begin{cases} \psi_{2q}(t), & t \leq 0.1 \\ (\psi_{1q}(0.3) - \psi_{2q}(0.1))(t - 0.1)/0.2 + \psi_{2q}(0.1), & 0.1 < t \leq 0.3 \\ \psi_{1q}(t), & 0.3 < t \end{cases} \tag{7}$$

where

$$\psi_{mq}(t) = 2\pi 10t + R_{mq}^{\mathrm{U}}(0, 2\pi) \tag{8}$$

and $R_{mq}^{\mathrm{U}}(0, 2\pi)$ denotes uniformly distributed random numbers from 0 to 2π with respect to m and q. $R_{mq}^{\mathrm{U}}(0, 2\pi)$ is the initial phase difference. The phases of channel 2 are connected to those of channel 1 with straight lines for the duration from 0.1 to 0.3 s, as shown in the top row of Fig. 2. These phase connections are random because of $R_{mq}^{\mathrm{U}}(0, 2\pi)$. Thus, the phases of channel 2 are unilaterally drawn into those of channel 1. Finally, the alpha-band activities are constructed as

$$x_{mq}^{\alpha}(t) = R_{mq}^{\mathrm{N}}(1, 0.3)\cos\left(\theta_{mq}(t) + R_{mqt}^{\mathrm{N}}(0, 0.3\pi)\right) \tag{9}$$

where $R_{mq}^{\mathrm{N}}(1, 0.3)$ and $R_{mqt}^{\mathrm{N}}(0, 0.3\pi)$ are amplitude-modulation and additive phase noise. The bottom row of Fig. 2 shows typical examples of given epochs of channels 1 and 2. These epochs are very noisy, so the stimulus-evoked activity cannot be observed directly.

The simulation was performed with a sampling frequency of 1 kHz.